Journal of the Brazilian Society of Mechanical Sciences and Engineering (2019) 41:135
https://doi.org/10.1007/s40430-019-1619-9

TECHNICAL PAPER

Impact of homogeneous–heterogeneous reactions and non-Fourier heat flux theory in Oldroyd-B fluid with variable conductivity

M. Irfan[1] · **M. Khan**[1] · **W. A. Khan**[2]

Received: 21 September 2018 / Accepted: 14 January 2019 / Published online: 18 February 2019

Abstract

This article scrutinizes the influence of chemical reactions on flow of an Oldroyd-B fluid due to stretched cylinder. In vision of non-Fourier heat flux model, the heat transfer phenomenon is scrutinized. This enhanced constitutive model anticipates the time space upper-convected derivative which is recycled to depicting heat conduction mechanism. Additionally, heat transfer scrutiny is considered with the influence of thermal conductivity which is temperature dependent. Apposite conversions are engaged to acquire ODEs which are then deciphered analytically via homotopic approach. To highlight their physical consequences, the graphical portrayal of diverse considerations on velocity, temperature and concentration fields is depicted and conferred. It is scrutinized from this study that all the profiles are higher in the instance of the cylinder as equated to a flat plate. This scrutiny also reported that the thermal relaxation parameter decreases the temperature field while the Schmidt number and homogeneous response parameter display the conflicting performance on concentration field. In addition, an assessment in restrictive instance is also presented in this exploration, which ensures us that our outcomes are more precise.

Keywords Oldroyd-B fluid · Variable thermal conductivity · Non-Fourier heat flux relation · Homogeneous–heterogeneous reactions · Stretching cylinder

List of symbols

(u, w)	Axial and radial velocity components
(r, z)	Space coordinates
(λ_1, λ_2)	Thermal relaxation and retardation times
v	Kinematic viscosity
U_0	Reference velocity
l	Characteristic length
R	Radius of cylinder
q	Heat flux
T	Temperature
$K(T)$	Variable thermal conductivity
k_∞	Thermal conductivity far away from stretched surface
T_w	Wall temperature
T_∞	Ambient temperature
δ_E	Thermal relaxation time of heat flux
(ρ_p, c_p)	Liquid density and specific heat at constant pressure
α_1	Thermal diffusivity
(G, H)	Chemical reactants
(g, h)	Concentration of chemical reactants
(k_c, k_s)	Rate constants
(D_G, D_H)	Diffusion of chemical reactants
g_0	Uniform concentration
λ^*	Ratio of diffusion coefficient
$w(z, r), u(z, r)$	Stretching velocities
α	Curvature parameter
(β_1, β_2)	Deborah numbers
ε	Thermal conductivity
Pr	Prandtl number
γ	Thermal relaxation parameter
Sc	Schmidt number
k_1, k_2	Measures of the strength of homogeneous–heterogeneous
η	Dimensionless variable
f	Dimensionless velocity
θ	Dimensionless temperature
l	Dimensionless concentration

Technical Editor: Cezar Negrao, PhD.

✉ M. Irfan
mirfan@math.qau.edu.pk

[1] Department of Mathematics, Quaid-i-Azam University, Islamabad 44000, Pakistan

[2] Department of Mathematics, Mohi-Ud-Din Islamic University, Nerian Sharif Azad Jammu and Kashmir, Pakistan

Abbreviations

ODEs	Ordinary differential equations
PDEs	Partial differential equations

1 Introduction

In all over the world, enthused researchers have recently exposed countless attention in scrutinizing the heat transfer phenomenon as a wave instead of diffusion because of its abundant engineering solicitations like cooling of energy invention, magnetic pills pursuing, biomedical applications and atomic vessels for cooling resolutions. The heat transfer is an extensive phenomenon in the nature which subsists owing to dissimilarity of temperature between entities or inside the similar body. For the former two spans, Fourier law of heat transfer [1] has been the only benchmark to estimate the heat transfer amount. The crucial downside of this law termed Paradox of heat conduction was to raise parabolic energy equation which designates that any distraction in the start will transmit all through the material. Cattaneo [2] intersected this obstacle by inserting relaxation time to heat flux. Moreover, this array was enhanced by Christov [3] by changing the material invariant sort of Maxwell–Cattaneo law by exhausting the Oldroyd's upper convective derivative. Hayat et al. [4] reported the performance of Cattaneo–Christov heat flux theory in variable thicked surface with variable conductivity. Ali and Sandeep [5] addressed the characteristics of an enhanced heat conduction relation on radiative magneto Casson-ferrofluid numerically. An Oldroyd-B fluid in the rotating frame by utilizing a developed heat conduction and mass diffusion relations was studied by Khan et al. [6]. They investigated that for rotation parameter both the primary and secondary velocities decline. Mustafa et al. [7] explored the aspects of thermal conductivity which is time dependent and non-Fourier heat flux concept in rotating structure of Maxwell fluid. They described that owing to insertion of elastic properties the hydrodynamic boundary layer befits thinner. Additional present-day endeavors in this aptitude are reported in references [8–12].

The growths of chemical species in the world arise through both heterogeneous/homogeneous responses. Recently, the technologists and engineers exhibit their thoughtful curiosity on analyzing new catalytic progressions functional at high temperature. Deprived of the exploitation of a catalyst, numerous reactions progress are very leisurely or insignificant. Heterogeneous/homogeneous responses are very compact which comprise the reduction and fabrication of reacting species at diverse amounts on the catalyst surfaces and within the liquids. A homogeneous reaction ensues where reactions and catalyst function in the similar phase; however, the heterogeneous reaction proceeds a limited area. Moreover, there are frequent chemically retorting structures containing both heterogeneous/homogeneous responses such as catalysis, organic systems and ignition. In addition, the significance of chemical species is more apparent in diverse industrial solicitations such as nutrition indulgence, fog materialization and diffusion, design of chemical dispensation apparatus, hydrometallurgical diligence, temperature distribution and vapor over cultivated lands and fruit tree plantations. Chaudhary and Merkin [13] investigated the features of heterogeneous/homogeneous reactions on viscous fluid with the stagnation point flow. Later on, for the study of the viscous liquid subject to heterogeneous/homogeneous reactions an isothermal model was suggested by Merkin [14]. Xu [15] studied the impact of chemical reactions in the stagnation region for heat fluid flow. He achieved multiple elucidations numerically with the aid of hysteresis bifurcations. Hayat et al. [16] scrutinized the chemical reactions on flow of a nanofluid with variable thicknesses. They investigated that the heat transfer amount decreases for Reynolds number. They noted that because of surface reaction this mechanism is dominant. The aspects of chemical species on generalized Burgers liquids were reported by Khan et al. [17]. Numerically the characteristics of convectively heated Riga plate on Williamson nanofluid by utilizing chemical reaction were explored by Ramzan et al. [18]. They detected that both Brownian motion and chemical reaction parameters are diminishing function of concentration field. Some additional current endeavors in this capacity are raised to references ([19–24]).

The analysis of liquid flow and heat transfer features of nonlinear materials has attracted the hurrying curiosity of the current researchers owing to the circumstance that most of nonlinear materials have more profuse scientifically and industrial solicitations instead of Newtonian materials [25–28]. The polymeric liquids, honey solutions, energy slurries, splatters, paper invention, oil retrieval and an assortment of soils are numerous specimens of nonlinear materials. It is quite awkward to increase a solitary constitutive correlation that foresees the assets of these constituents because the nature of these resources is very multifaceted and intricate. For instance, the heat transport properties on nonlinear materials axisymmetric channel via parameterized perturbation technique was analyzed by Ashorynejad et al. [29] An Oldroyd-B fluid by using nanoparticles with combined stratification was examined by Waqas et al. [30]. They establish that the temperature and mass stratification decline the temperature and concentration fields. The impact of the heat sink/source on unsteady radiative flow of Williamson liquid was reported by Khan and Hamid [31]. In their exploration, they initiated that the heat transfer enhances for higher thermal radiation and temperature ratio parameter. Sandeep [32] observed the influence of aligned magnetic field on nanoliquid with graphene nanoparticles. He noticed that aligned magnetic field normalizes the local Nusselt number; however, the thermal conductivity of water increases for intensifying values of volume fraction of nanoparticles. Additionally, to envision their sufficient performance numerous constitutive

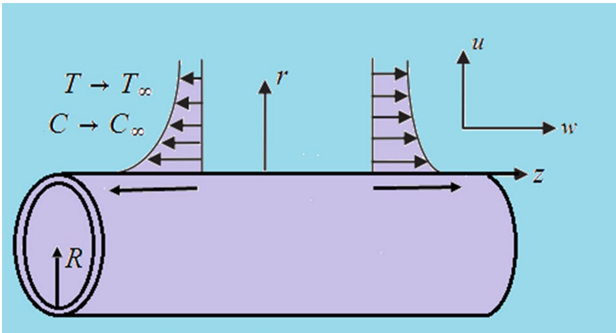

Fig. 1 Schematic diagram

interactions have been established for non-Newtonian liquids [33–41].

Stimulated by all the aforesaid fiction and countless prospective developed and industrial anxieties, the notable concern of this scrutiny is sightseeing the notion of an improved heat conduction and chemical species on an Oldroyd-B fluid flow caused by a stretched cylinder. Additionally, variable thermal conductivity is presented for the heat transfer purpose. Apposite alteration changes the PDEs into nonlinear ODEs which are then elucidated analytically by means of homotopic scheme. Moreover, the flow structures are scrutinized for assorted scheming parameters graphically and conferred in detail.

2 Mathematical formulations

The mathematical framing of the current flow analysis is in the following three subdivisions.

2.1 Flow equation

We consider the steady 2D axisymmetric flow of an Oldroyd-B fluid influenced by a stretched cylinder of radius R. The cylinder is stretching with velocity $\frac{U_0 z}{l}$, along z-direction, where $(U_0,\ l)$ is the reference velocity and characteristic length, respectively. Let the cylindrical polar coordinates $(r,\ z)$ be engaged in such a way that z-axis is adjacent to the axis of the cylinder and r-axis is restrained near the radial direction (as depicted in Fig. 1). The continuity and momentum equations of the flow analysis are as follows [42, 43]:

$$\frac{\partial u}{\partial r} + \frac{u}{r} + \frac{\partial w}{\partial z} = 0, \tag{1}$$

$$u\frac{\partial w}{\partial r} + w\frac{\partial w}{\partial z} + \lambda_1\left[w^2\frac{\partial^2 w}{\partial z^2} + u^2\frac{\partial^2 w}{\partial r^2} + 2uw\frac{\partial^2 w}{\partial r\partial z}\right] = \nu\left[\frac{\partial^2 w}{\partial r^2} + \frac{1}{r}\frac{\partial w}{\partial r}\right]$$
$$+ \nu\lambda_2\left[\frac{u}{r^2}\frac{\partial w}{\partial r} - \frac{1}{r}\frac{\partial w}{\partial r}\frac{\partial w}{\partial z} - \frac{2}{r}\frac{\partial u}{\partial r}\frac{\partial w}{\partial r} + \frac{w}{r}\frac{\partial^2 w}{\partial r\partial z} - \frac{\partial w}{\partial r}\frac{\partial^2 w}{\partial r\partial z} - 2\frac{\partial w}{\partial r}\frac{\partial^2 u}{\partial r^2} + \frac{u}{r}\frac{\partial^2 w}{\partial r^2} - \frac{\partial w}{\partial z}\frac{\partial^2 w}{\partial r^2} + w\frac{\partial^3 w}{\partial r^2\partial z} + u\frac{\partial^3 w}{\partial r^3}\right], \tag{2}$$

subject to boundary conditions

$$w(R,z) = W(z) = \frac{U_0 z}{l}, \quad u(R,z) = 0, \tag{3}$$

$$w \to 0, \quad \text{as} \quad r \to \infty. \tag{4}$$

Here, $(u,\ w)$ are the velocity components in r- and z-directions, respectively, ν the kinematic viscosity and $\lambda_i\,(i = 1,\ 2)$ the thermal relaxation and retardation times.

Considering the conversions

$$u = -\frac{R}{r}\sqrt{\frac{U_0\nu}{l}}f(\eta),\ \ w = \frac{U_0 z}{l}f'(\eta),\ \ \eta = \sqrt{\frac{U_0}{\nu l}}\left(\frac{r^2 - R^2}{2R}\right), \tag{5}$$

Equation (1) is satisfied automatically, and Eqs. (2)–(4) yield

$$(1 + 2\alpha\eta)f''' + 2\alpha f'' + ff'' - f'^2 + 2\beta_1 f'ff'' - \beta_1 f^2 f'''$$
$$- \frac{\alpha\beta_1}{(1 + 2\alpha\eta)}f^2 f'' + (1 + 2\alpha\eta)\beta_2(f''^2 - ff^{iv}) - 4\alpha\beta_2 ff''' = 0, \tag{6}$$

$$f(0) = 0,\ f'(0) = 1,\ f'(\infty) = 0. \tag{7}$$

Here, $\alpha\left(= \frac{1}{R}\sqrt{\frac{\nu l}{U_0}}\right)$ is the curvature parameter and $\beta_i\left(= \frac{\lambda_i U_0}{l}\right)(i = 1,\ 2)$ the Deborah numbers.

2.2 Energy equation

The equation of energy for this circumstance is

$$(\rho c)_p\left(u\frac{\partial T}{\partial r} + w\frac{\partial T}{\partial z}\right) = -\nabla \cdot \mathbf{q}, \tag{8}$$

where T is the liquid temperature, $(\rho_p,\ c_p)$ the liquid density and specific heat at constant pressure, respectively, and $\mathbf{q}$ the heat flux. In the vision of Cattaneo–Christov, the heat flux satisfies

$$\mathbf{q} + \delta_E\left(\frac{\partial \mathbf{q}}{\partial t} + \mathbf{V}\cdot\nabla\mathbf{q} - \mathbf{q}\cdot\nabla\mathbf{V} + (\nabla\cdot\mathbf{V})\mathbf{q}\right) = -K(T)\nabla T, \tag{9}$$

where δ_E is the thermal relaxation time of heat flux and $K(T)$ the thermal conductivity which is temperature dependent.

For incompressibility condition, the above equation yields

$$\mathbf{q} + \delta_E\left(\frac{\partial \mathbf{q}}{\partial t} + \mathbf{V}\cdot\nabla\mathbf{q} - \mathbf{q}\cdot\nabla\mathbf{V}\right) = -K(T)\nabla T. \tag{10}$$

By eliminating **q** from Eqs. (8) and (10), we finally have

$$u\frac{\partial T}{\partial r}+w\frac{\partial T}{\partial z}+\delta_E\left[\begin{array}{c} w^2\frac{\partial^2 T}{\partial z^2}+u^2\frac{\partial^2 T}{\partial r^2}+2uw\frac{\partial^2 T}{\partial z\partial r} \\ \left(w\frac{\partial w}{\partial z}+u\frac{\partial u}{\partial r}\right)\frac{\partial T}{\partial z}+\left(w\frac{\partial u}{\partial z}+u\frac{\partial u}{\partial r}\right)\frac{\partial T}{\partial r}\end{array}\right] = \frac{1}{(\rho c)_p r}\frac{\partial}{\partial r}\left[K(T)r\frac{\partial T}{\partial r}\right], \tag{11}$$

with boundary conditions

$$T=T_w \text{ at } r=R \text{ and } T\to T_\infty, \text{ as } r\to\infty. \tag{12}$$

Here, (T_w, T_∞) are the wall and ambient temperatures, respectively, and $K(T)$ the temperature-dependent thermal conductivity, which is defined as

$$K(T)=k_\infty\left[1+\varepsilon\left(\frac{T-T_\infty}{\Delta T}\right)\right], \tag{13}$$

where (k_∞, ε) are the thermal conductivity and small scale parameter, respectively, and ΔT the difference between the liquid temperature of stretched surface and far away from the surface of cylinder.

The non-dimensional temperature of Oldroyd-B liquid is defined by the following relation:

$$\theta(\eta)=\frac{T-T_\infty}{T_w-T_\infty}. \tag{14}$$

Substituting Eqs. (13) and (14) in Eqs. (11) and (12) we have

$$(1+2\alpha\eta)\theta''+2\alpha\theta'+(1+2\alpha\eta)(\theta\theta''+\theta'^2)\varepsilon + 2\alpha\varepsilon\theta\theta'-\Pr\gamma(ff'\theta'+\gamma f^2\theta''), \tag{15}$$

$$\theta(0)=1 \quad \text{and} \quad \theta(\infty)=0. \tag{16}$$

Here, $\gamma\left(=\frac{\delta_E U_0}{l}\right)$ is the thermal relaxation factor and $\Pr\left(=\frac{\nu}{\alpha_1}\right)$ the Prandtl number.

2.3 Relation for the chemical species

The interaction between heterogeneous and homogeneous responses consists of chemical reactants (G, H) which have the concentrations (g, h) and rate constants (k_c, k_s). Also, the isothermal response heterogeneous (surface) of the first order is of the form

$$G+2H\to 3H, \quad \text{rate}=k_c g h^2, \tag{17}$$

$$G\to H, \quad \text{rate}=k_s g. \tag{18}$$

Moreover, an assumption is made that both the reactions are isothermal and distant from the sheet at the ambient fluid; for reactant G, there is a uniform concentration g_0 while there is no autocatalyst H.

Under these attentions, the equations of chemical species with boundary conditions are

$$u\frac{\partial g}{\partial r}+w\frac{\partial g}{\partial z}=D_G\left(\frac{1}{r}\frac{\partial g}{\partial r}+\frac{\partial^2 g}{\partial r^2}\right)-k_c g h^2, \tag{19}$$

$$u\frac{\partial h}{\partial r}+w\frac{\partial h}{\partial z}=D_H\left(\frac{1}{r}\frac{\partial h}{\partial r}+\frac{\partial^2 h}{\partial r^2}\right)+k_c g h^2, \tag{20}$$

$$D_G\frac{1}{r}\frac{\partial g}{\partial r}=k_s g,\ D_H\frac{1}{r}\frac{\partial h}{\partial r}=-k_s g \ at\ r=R, \tag{21}$$

$$g\to g_0, \quad h\to 0 \text{ as } r\to\infty, \tag{22}$$

where (D_G, D_H) are the coefficients of diffusion species G and H, respectively.

Under the following conversions

$$g=g_0 l(\eta),\ h=h_0 m(\eta), \tag{23}$$

Transformations of Eqs. (19)–(22) yield

$$\frac{(1+2\alpha\eta)}{Sc}l''+fl'-k_1 l m^2=0, \tag{24}$$

$$\frac{\lambda^*(1+2\alpha\eta)}{Sc}m''+fm'+k_1 l m^2=0, \tag{25}$$

$$l'(0)=k_2 l(0),\ \ \lambda^* m'(0)=-k_2 l(0), \tag{26}$$

$$l\to 1,\ \ m\to 0\ as\ \eta\to\infty. \tag{27}$$

In the above equations, $\lambda^*\left(=\frac{D_H}{D_G}\right)$ is the ratio of the diffusion coefficient, (k_2, k_1) the measures of the strength of heterogeneous–homogeneous processes and $Sc\left(=\frac{\nu}{D_G}\right)$ the Schmidt number.

According to assumption, the diffusion coefficients D_G and D_H are taken to be equivalent, i.e., $\lambda^*=1$, and we obtained

$$l(\eta)+m(\eta)=1. \tag{28}$$

Thus, we have the following equation with boundary conditions

$$\frac{(1+2\alpha\eta)}{Sc}l''+fl'-k_1(1-l)^2 l=0, \tag{29}$$

$$l'(0)=k_2 l(0),\ \ l\to 1 \text{ as } \eta\to\infty. \tag{30}$$

3 Physical interpretation

This crucial section is envisioned to visualize the stimulus of essential somatic parameters on velocity, temperature and concentration fields via homotopic approach. For this purpose, graph is portrayed and conferred in detail. Furthermore, Table 1 shows $-f''(0)$ in limiting sense. This table contributes the assessment of up-to-date outcomes with the present prose with excellent agreement.

3.1 Velocity field

Figure 2a, b is plotted to clarify the features of Deborah numbers β_1 and β_2 on the velocity field. From these sketches, we noted that the liquid velocity displays the conflicting tendency for β_1 and β_2. The higher values of β_1 specify that the stress relaxation is unhurried as related to the timescale scrutiny. This means that the liquid exhibits solid-like reaction when subjected to the applied stress, and hence, the liquid velocity declines for β_1. It is also famed that the retardation time raises to the time required for the buildup of shear stress in a liquid. Therefore, it can be portrayed that the timescales are perceived throughout the start-up investigations that are not clarified by relaxation time. This shows that the liquid flow parallel to the sheet accelerates with an augmentation in liquid retardation time and hence the liquid velocity rises for β_2. In addition, we can also detect that the thickness of the momentum boundary layer is higher for the case flow over a cylinder when associated flow over a flat plate.

Table 1 An assessment value of $-f''(0)$ for numerous values of β_1 in limiting cases when $\alpha = \beta_2 = 0$

β_1	$-f''(0)$			
	Ref. [44]	Ref. [45]	Ref. [30]	Present
0.0	1.000000	0.999978	1.000000	1.0000000
0.1				1.0261837
0.2	1.051948	1.051945	1.051889	1.0518890
0.3				1.0771256
0.4	1.101850	1.101848	1.101903	1.1019035
0.5				1.1262357
0.6	1.150163	1.150160	1.150137	1.1501374
0.7				1.1736240
0.8	1.196692	1.196690	1.196711	1.1967114
0.9				1.2194143
1.0				1.2417477
1.2	1.285257	1.285253	1.285363	1.2853630
1.4				1.3276675
1.6	1.368641	1.368641	1.368758	1.3687582
1.8				1.4087264
2.0	1.447617	1.447616	1.447651	1.4476526

3.2 Temperature field

Figure 3a, b scrutinizes the impact of Deborah number β_2 and temperature-dependent thermal conductivity ε on the temperature field. Increasing values of β_2 and ε decline the temperature field for β_2, while it enhances for ε. It can be established that the depth of heat penetration decreases when liquid retardation time intensified which illustrates the reduction in liquid temperature for β_2. Moreover, the thermal conductivity of liquid boosts up when we increase ε. The higher thermal conductivity infers thicker the penetration depth and lesser the wall temperature gradient. Because of this circumstance, the liquid temperature of Oldroyd-B liquid is intensified.

The impact of progressive values of Prandtl number Pr and thermal relaxation time parameter γ is shown in Fig. 4a, b. Declining tendency of both the parameters for amassed values of Pr and γ is being noticed from these statistics. As an outcome, for advanced values of Prandtl number Pr we initiate a thinner thickness of the thermal boundary layer with better quality wall slope

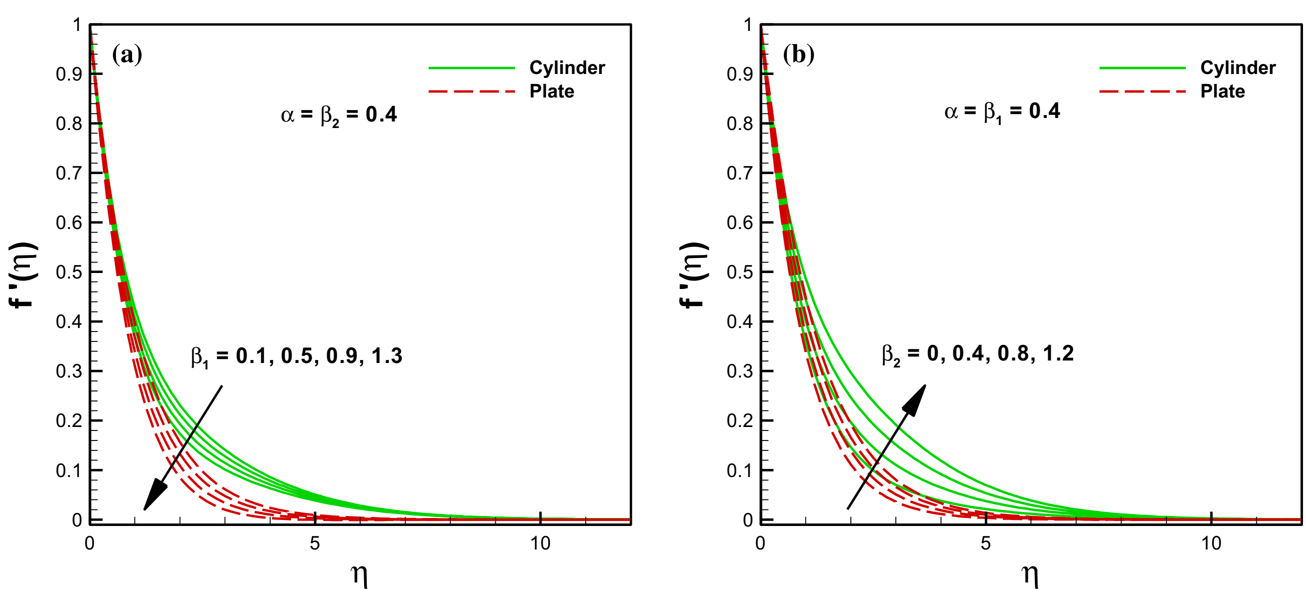

Fig. 2 Impact of Deborah numbers β_1 and β_2 on velocity field

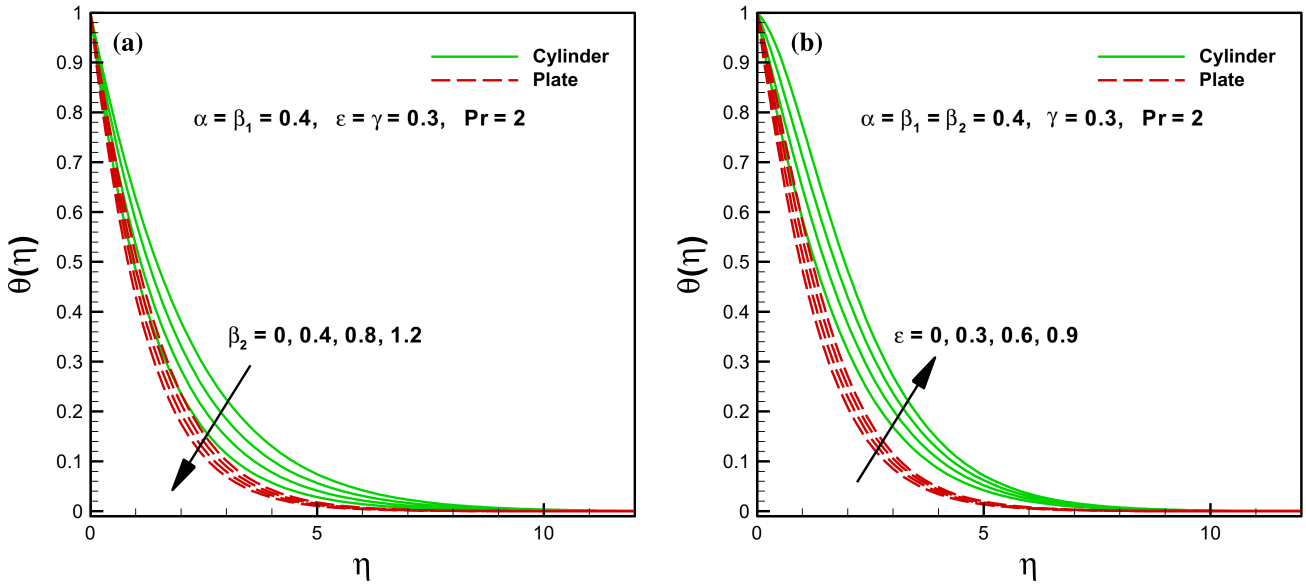

Fig. 3 Impact of Deborah numbers β_2 and thermal conductivity parameter ε on temperature field

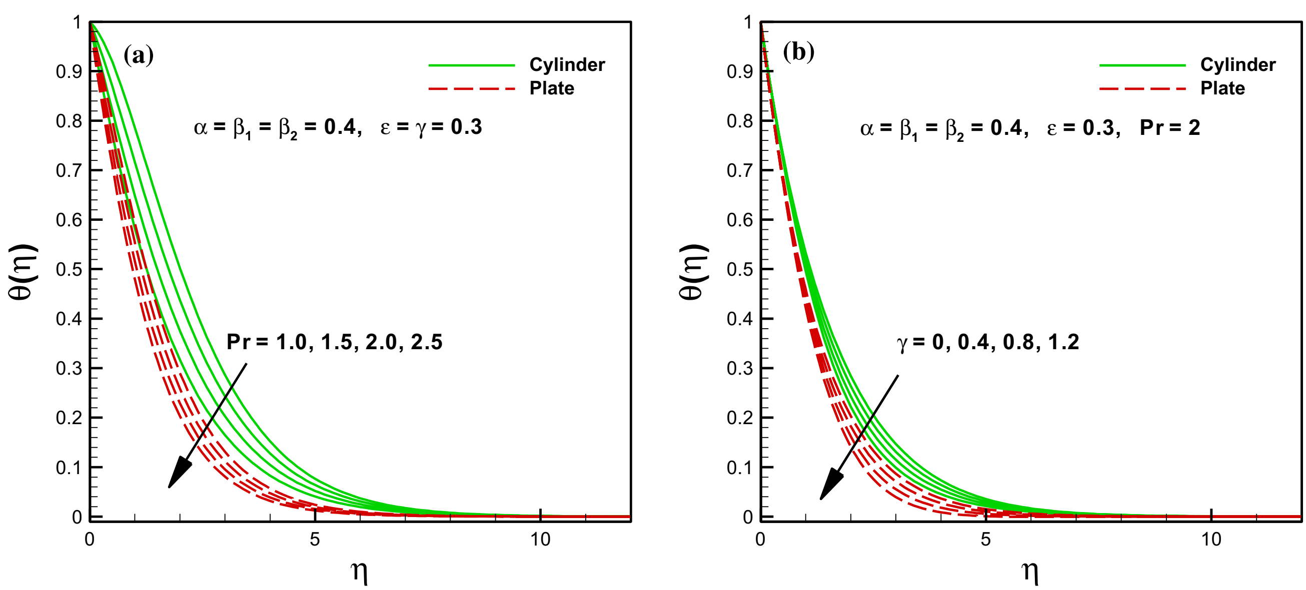

Fig. 4 Impact of Prandtl number Pr and thermal relaxation parameter γ on temperature field

of temperature. Hence, the temperature field decreases. From Fig. 4b, similar outcomes are being identified for higher values of γ. When we enlarges γ, a non-conducting behavior of particles appears, which is liable to decline in the temperature field for both $\alpha = 0$ (sheet) and $\alpha \neq 0$ (cylinder).

3.3 Concentration field

Figure 5a, b shows the stimulus of homogeneous–heterogeneous parameters (k_1, k_2) on concentration field for both cylinder and sheet cases. For escalation in these parameters exhibits conflicting drift on concentration field. It is exposed that the concentration decreases as the strength k_1 of homogeneous response increases. It is also known that the concentration field is a diminishing function of the asset of heterogeneous response k_2. Physically, the

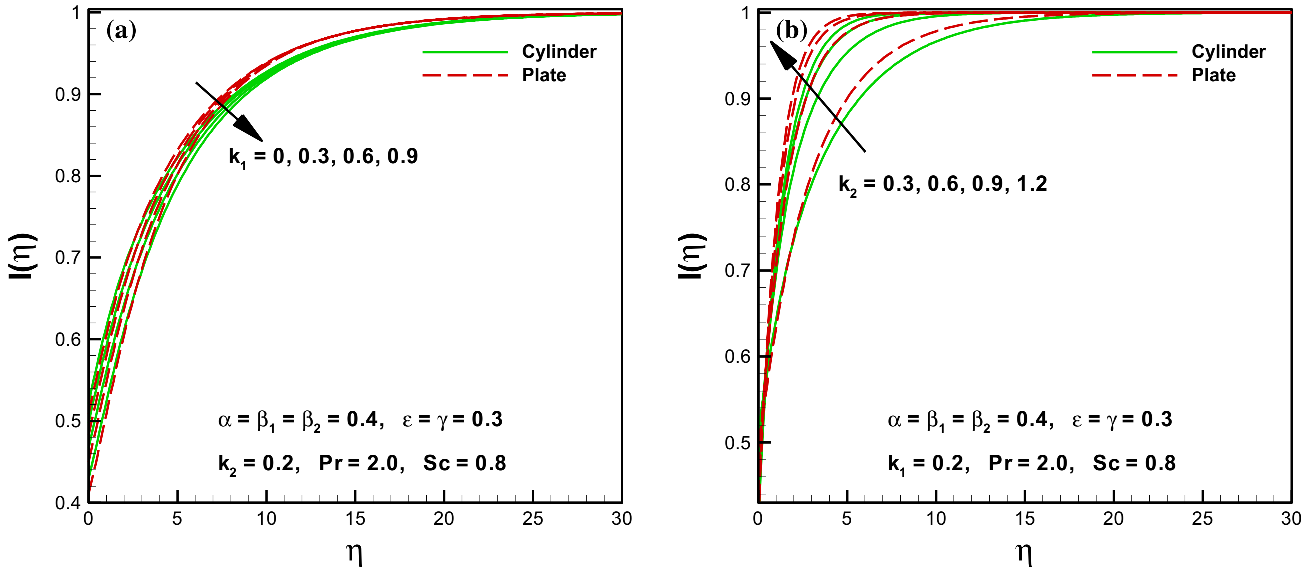

Fig. 5 Impact of homogeneous response parameter k_1 and heterogeneous response parameter k_2 on concentration field

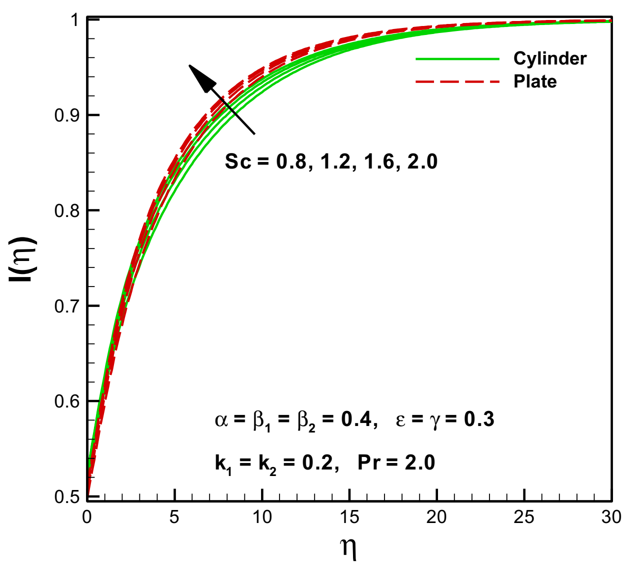

Fig. 6 Impact of Schmidt number *Sc* on concentration field

reactants are consumed through the homogeneous response which causes a decrease in the concentration field.

Figure 6 shows the impact of higher value of Schmidt number *Sc* on concentration field. Augmenting behavior of concentration field is being detected for the progressive values of *Sc* on Oldroyd-B liquid. This is owing to the point that Schmidt number *Sc* is the proportion of momentum diffusivity to mass diffusivity and as an outcome advanced values of Schmidt number *Sc* resemble the lesser mass diffusivity. Hence, the concentration field decreases.

4 Concluding remarks

The analytical elucidations have been executed for the exploration of an Oldroyd-B liquid in the manifestation of Cattaneo–Christov heat conduction relation and chemical reactions. The temperature-dependent thermal conductivity is also presented. The current investigation demonstrated the following noteworthy facts:

- It can be inferred that the liquid velocity exhibits conflicting tendency for augmented values of Deborah numbers β_1 and β_2.
- The liquid temperature declines with increasing values of the thermal relaxation parameter γ, while analogous impact is being noticed for the thermal conductivity parameter ε.
- The Schmidt number *Sc* and heterogeneous reaction parameter k_2 enhances the concentration field, but the tendency of homogeneous reaction parameter k_1 is quite reversed for the concentration of Oldroyd-B liquid.

References

1. Fourier JBJ (1822) Theorie analytique de la chaleur. Elsevier, Paris
2. Cattaneo C, Calore SCD, Semin A (1948) Sulla conduzione del calore. Mat Fis Univ Modena Reggio Emilia 3:83–101
3. Christov CI (2009) On frame indifferent formulation of the Maxwell–Cattaneo model of finite-speed heat conduction. Mech Res Commun 36:481–486

4. Hayat T, Khan MI, Farooq M, Alsaedi A, Waqas M, Yasmeen T (2016) Impact of Cattaneo–Christov heat flux model in flow of variable thermal conductivity fluid over a variable thicked surface. Int J Heat Mass Transf 99:702–710
5. Ali ME, Sandeep N (2017) Cattaneo–Christov model for radiative heat transfer of magnetohydrodynamic Casson-ferrofluid: a numerical study. Results Phys 7:21–30
6. Khan WA, Irfan M, Khan M (2017) An improved heat conduction and mass diffusion models for rotating flow of an Oldroyd-B fluid. Results Phys 7:3583–3589
7. Mustafa M, Hayat T, Alsaedi A (2017) Rotating flow of Maxwell fluid with variable thermal conductivity: an application to non-Fourier heat flux theory. Int J Heat Mass Transf 106:142–148
8. Waqas M, Khan MI, Hayat T, Alsaedi A, Khan MI (2017) On Cattaneo–Christov double diffusion impact for temperature-dependent conductivity of Powell-Eyring liquid. Chin J Phys 55:729–737
9. Mahanthesh B, Makinde OD, Gireesha BJ, Krupalakshmi KL, Animasaun IL (2018) Two-Phase flow of dusty Casson fluid with Cattaneo–Christov heat flux and heat source past a cone, wedge and plate. Defect Diffus Forum 387:625–639
10. Irfan M, Khan M, Khan WA (2018) Interaction between chemical species and generalized Fourier's law on 3D flow of Carreau fluid with variable thermal conductivity and heat sink/source: a numerical approach. Results Phys 10:107–117
11. Upadhya SM, Raju CSK, Mahesha, Saleem S (2018) Nonlinear unsteady convection on micro and nanofluids with Cattaneo–Christov heat flux. Results Phys 9:779–786
12. Khan M, Irfan M, Khan WA, Ayaz M (2018) Aspects of improved heat conduction relation and chemical processes on 3D Carreau fluid flow. Pramana J Phys 91:14. https://doi.org/10.1007/s12043-018-1579-0
13. Chaudhary MA, Merkin JH (1995) A simple isothermal model for homogeneous–heterogeneous reactions in boundary-layer flow. I equal diffusivities. Fluid Dyn Res 16:311–333
14. Merkin JH (1996) A model for isothermal homogeneous–heterogeneous reactions in boundary layer flow. Math Comput Model 24:125–136
15. Xu H (2017) A homogeneous–heterogeneous reaction model for heat fluid flow in the stagnation region of a plane surface. Int Commun Heat Mass Transf 87:112–117
16. Hayat T, Rashid M, Imtiaz M, Alsaedi A (2017) Nanofluid flow due to rotating disk with variable thickness and homogeneous–heterogeneous reactions. Int J Heat Mass Transf 113:96–105
17. Khan WA, Irfan M, Khan M, Alshomrani AS, Alzahrani AK, Alghamdi MS (2017) Impact of chemical processes on magneto nanoparticle for the generalized Burgers fluid. Int J Mol Liq 234:201–208
18. Ramzan M, Bilal M, Chung JD (2017) Radiative Williamson nanofluid flow over a convectively heated Riga plate with chemical reaction-A numerical approach. Chin J Phys 55:1663–1673
19. Khan MI, Waqas M, Hayat T, Khan MI, Alsaedi A (2017) Numerical simulation of nonlinear thermal radiation and homogeneous–heterogeneous reactions in convective flow by a variable thicked surface. J Mol Liq 246:259–267
20. Gireesha BJ, Kumar PBS, Mahanthesh B, Shehzad SA, Rauf A (2017) Nonlinear 3D flow of Casson-Carreau fluids with homogeneous–heterogeneous reactions: a comparative study. Results Phys 7:2762–2770
21. Kumar R, Sood S, Sheikholeslami M, Shehzad SA (2017) Nonlinear thermal radiation and cubic autocatalysis chemical reaction effects on the flow of stretched nanofluid under rotational oscillations. J Colloid Interface Sci 505:253–265
22. Khan M, Irfan M, Khan WA (2018) Thermophysical properties of unsteady 3D flow of magneto Carreau fluid in presence of chemical species: a numerical approach. J Braz Soc Mech Sci Eng 40:108. https://doi.org/10.1007/s40430-018-0964-4
23. Hayat T, Rashid M, Alsaedi A (2018) Three dimensional radiative flow of magnetite-nanofluid with homogeneous–heterogeneous reactions. Results Phys 8:268–275
24. Kumar R, Kumar R, Sheikholeslami M, Chamkha AJ (2019) Irreversibility analysis of the three dimensional flow of carbon nanotubes due to nonlinear thermal radiation and quartic chemical reactions. J Mol Liq 274:379–392
25. Sheikholeslami M, Ganji DD, Rashidi MM (2016) Magnetic field effect on unsteady nanofluid flow and heat transfer using Buongiorno model. J Mag Mag Mater 416:164–173
26. Sheikholeslami M (2018) Influence of magnetic field on Al2O3–H2O nanofluid forced convection heat transfer in a porous lid driven cavity with hot sphere obstacle by means of LBM. J Mol Liq 263:472–488
27. Sheikholeslami M, Jafaryar M, Li Z (2018) Second law analysis for nanofluid turbulent flow inside a circular duct in presence of twisted tape turbulators. J Mol Liq 263:489–500
28. Sheikholeslami M (2018) Application of Darcy law for nanofluid flow in a porous cavity under the impact of Lorentz forces. J Mol Liq 266:495–503
29. Ashorynejad HR, Javaherdeh K, Sheikholeslami M, Ganji DD (2014) Investigation of the heat transfer of a non-Newtonian fluid flow in an axisymmetric channel with porous wall using parameterized perturbation method (PPM). J Frankl Inst 35:701–712
30. Waqas M, Khan MI, Hayat T, Alsaedi A (2017) Stratified flow of an Oldroyd-B nanoliquid with heat generation. Results Phys 7:2489–2496
31. Khan M, Hamid A (2017) Influence of non-linear thermal radiation on 2D unsteady flow of a Williamson fluid with heat source/sink. Results Phys 7:3968–3975
32. Sandeep N (2017) Effect of aligned magnetic field on liquid thin film flow of magnetic-nanofluids embedded with graphene nanoparticles. Adv Powder Technol 28:865–875
33. Khan AA, Ellahi R, Gulzar MM, Sheikholeslami M (2014) Effects of heat transfer on peristaltic motion of Oldroyd fluid in the presence of inclined magnetic field. J Mag Mag Mater 372:97–106
34. Haq RU, Hamouch Z, Hussain ST, Mekkaoui T (2017) MHD mixed convection flow along a vertically heated sheet. Int J Hydro Energy 45:15925–15932
35. Ellahi R, Bhatti MM, Khalique CM (2017) Three-dimensional flow analysis of Carreau fluid model induced by peristaltic wave in the presence of magnetic field. Int J Mol Liq 241:1059–1068
36. Khan M, Irfan M, Khan WA, Alshomrani AS (2017) A new modeling for 3D Carreau fluid flow considering nonlinear thermal radiation. Results Phys 7:2692–2704
37. Anwar MS, Rasheed A (2017) Simulations of a fractional rate type nanofluid flow with non-integer Caputo time derivatives. Comput Math Appl 74:2485–2502
38. Irfan M, Khan M, Khan WA (2018) On model for three-dimensional Carreau fluid flow with Cattaneo-Christov double diffusion and variable conductivity: A numerical approach. J Braz Soc Mech Sci Eng 40:577. https://doi.org/10.1007/s40430-018-1498-5
39. Hayat T, Rashid M, Khan MI, Alsaedi A (2018) Melting heat transfer and induced magnetic field effects on flow of water based nanofluid over a rotating disk with variable thickness. Results Phys 9:1618–1630
40. Domairry D, Sheikholeslami M, Ashorynejad HR, Gorla RSR, Khani M (2012) Natural convection flow of a non-Newtonian nanofluid between two vertical flat plates. Proc Inst Mech Eng Part N J Nanoeng Nanosyst 225:115–122
41. Khan M, Ahmed J, Ahmad L (2018) Chemically reactive and radiative von Kármán swirling flow due to a rotating disk. Appl Math Mech 39:1295–1310
42. Irfan M, Khan M, Khan WA (2018) Impact of non-uniform heat sink/source and convective condition in radiative heat transfer to

Oldroyd-B nanofluid: a revised proposed relation. Phys Lett A 383:376–382. https://doi.org/10.1016/j.physleta.2018.10.040

43. Irfan M, Khan M, Khan WA, Sajid M (2018) Thermal and solutal stratifications in flow of Oldroyd-B nanofluid with variable conductivity. Appl Phys A 383:376–382. https://doi.org/10.1007/s00339-018-2086-3
44. Abel MS, Tawade JV, Nandeppanavar MM (2012) MHD flow and heat transfer for the upper-convected Maxwell fluid over a stretching sheet. Meccanica 47:385–393
45. Megahed AM (2013) Variable fluid properties and variable heat flux effects on the flow and heat transfer in a non-Newtonian Maxwell fluid over an unsteady stretching sheet with slip velocity. Chin Phys B 22:094701